Water and sediment exchange between the anthropogenically modified distributaries of the Yangtze Estuary

Zhu, Chunyan; van Maren, D. S.; Guo, Leicheng; Xie, Weiming; Xing, Chaofeng; Wang, Zheng Bing; He, Qing

DOI
10.1016/j.catena.2025.108729

Publication date
2025

Document Version
Final published version

Published in
Catena

Catena 250 (2025) 108729

Contents lists available at ScienceDirect

Catena

journal homepage: www.elsevier.com/locate/catena

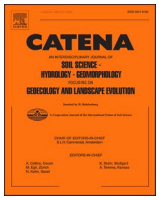

Water and sediment exchange between the anthropogenically modified distributaries of the Yangtze Estuary

Chunyan Zhu [a], D.S. van Maren [b,c], Leicheng Guo [a], Weiming Xie [a], Chaofeng Xing [a,d], Zheng Bing Wang [b,c], Qing He [a,*]

[a] State Key Laboratory of Estuarine and Coastal Research, East China Normal University, Shanghai 200241, China
[b] Faculty of Civil Engineering and Geosciences, Delft University of Technology, Delft 2600GA, the Netherlands
[c] Deltares, Delft, the Netherlands
[d] Shanghai SICC Engineering Design Co., Ltd, Shanghai 200093, China

ARTICLE INFO

Keywords:
Sediment exchange
Navigation channel
Yangtze Estuary
Channel-shoal system
Engineering works
Delta development

ABSTRACT

Human interventions influence sediment dynamics, and understanding these mechanisms is essential for predicting short-term and long-term estuarine development. The Deep Channel Navigation Project (DCNP) in the Yangtze Estuary is such a large infrastructural intervention that substantially alters sediment exchanges between channels and shoals and may thereby influence this estuarine development. However, the effect of these constructions on channel-shoal sediment exchange is up to now poorly known. In this study, we use an extensive dataset collected both in channels and on shoals and a numerical model to clarify the exchange mechanisms driving sediment transport patterns in a strongly anthropogenically modified environment. The results indicate that the stepwise construction of hydraulic structures leads to gradual changes in sediment exchange. The first phase was characterized by partially blocked sediment exchange with northward sediment transport towards the main channel and to the northern flats (2002–2010). Next, a transition period was characterized by weaker horizontal sediment exchange and reduced sediment supply (2010–2016). Since 2016, more efficient structures blocking sediment exchange further hinder northward transport and promote deposition on the southern flats. These processes point to the important role of engineering works in strengthening the southward growth of the delta. Moreover, data analyses suggest that northward over-jetty flow during high water induces a net sediment flux towards the channel due to water level gradients. The residual flow controls the net sediment transport both in the longitudinal and lateral direction over the tidal flats. Therefore, a clockwise residual circulation cell forms in the channel-shoal system, contributing to the channel siltation. These findings shed important insights into the role of sediment exchange in channel siltation and large-scale hydrodynamic and delta development. Such knowledge is crucial for sustainable future management of delta distributaries.

1. Introduction

Estuaries connect the sheltered fluvial system from the exposed open coast, providing crucial economic functions (shipping, freshwater availability), ecological functions (providing essential habitats for numerous species) and safety against flooding. The dynamics of these systems are strongly influenced by water and sediment exchange processes, both on a large scale (linking the fresh water and marine environment) and on smaller scales (between channels and shoals). Exchange of water and sediment drives bed level changes and therefore the navigational functions for shipping industry as well as regulating ecological functions (exchanging nutrients, heavy metals, and other materials (Liu et al., 2022). Therefore, understanding water and sediment exchange processes is essential for estuarine morphological and ecological development.

Water and sediment exchange processes generate spatial gradients in residual sediment transport which in turn control estuarine erosion and deposition rates and patterns. In the longitudinal direction, estuarine circulation (characterized by a seaward residual flow near the surface and a landward residual flow near the bottom) leads to sediment trapping and formation of turbidity maximum, with time scales typically varying over seasonal and spring-neap tidal cycles (Geyer and

* Corresponding author.
E-mail address: qinghe@sklec.ecnu.edu.cn (Q. He).

https://doi.org/10.1016/j.catena.2025.108729
Received 15 April 2024; Received in revised form 3 October 2024; Accepted 14 January 2025
Available online 5 February 2025

MacCready, 2014; Burchard et al., 2018). These longitudinal processes vary over the cross-section, with barotropic flow driving a net landward flow over the shallow banks compensated by a net seaward flow in the main channel while baroclinic processes may reverse this pattern, strongly influencing sediment exchanges in channel-shoal systems (Ralston et al., 2012; Lacy et al., 2014). Superimposed on these longitudinal processes are lateral processes (circulation, asymmetry, and advection) modulating exchange flows, stratification, and sediment trapping (Chen et al., 2020). In many engineered estuaries, these natural water and sediment exchange processes are further modulated by multiple human interventions. For instance, deepening and narrowing enhance flood-dominant tidal asymmetry and amplification and reduction in hydraulic drag and therefore enhance sediment trapping in the Ems, Loire, and Yangtze Estuary (Winterwerp and Wang, 2013; van Maren et al., 2015; Zhu et al., 2021a). Reclamation may enhance landward sediment transport and therefore channel infilling due to the loss of intertidal flats e.g., in the Hangzhou Bay and North Branch of the Yangtze Estuary (Xie et al., 2017a; Guo et al., 2022). Dredging and other estuarine modifications have altered bed shear stress, tidal asymmetry, and sediment pathways, e.g., in the Coos Bay Estuary for $>$ 150 years (Eidam et al., 2021). However, previous studies focus on a single channel system while many tidal-dominated estuaries are characterized by multiple distributaries (Hoitink et al., 2020; Nienhuis et al., 2020). In these multi-channel estuaries, sediment exchange processes play an important role in channel stability (Lenstra et al., 2019; van Maren et al., 2023a) and connectivity (Pearson et al., 2020; Hiatt et al., 2022), impacting large-scale and long-term delta evolution (Zhou et al., 2017).

The Yangtze Estuary is a multi-distributary system with four outlets driven by combined river and tidal forcing. The abundant riverine sediment discharge controls the long-term depositional development in the pre-2000 s whereas the sediment supply has been decreasing since the mid-1980 s which may decrease the sediment concentration within the estuary (Zhu et al., 2019; Juez et al., 2021; Guo et al., 2021). However, the mouth zone has sustained accretion with a time lag of decades in response to the sediment decline (Zhu et al., 2019). This is very likely contributed by sediment exchanges within the estuary where many large engineering works take place. One of the largest engineering works in the North Passage in the mouth zone is the Deep Channel Navigation Project (DCNP) which includes dredging activities and engineering structures (Fig. 1). Previous studies have documented that the DCNP has caused significant changes in the regional hydrodynamics and sediment dynamics, e.g., reinforced high near-bed suspended sediment concentrations (SSC) and siltation which are attributed to enhanced gravitational circulation due to channel deepening (Jiang et al., 2013; Lin et al., 2021). In turn, the high near-bed SSC introduces strong sediment-induced density effects which further enhance stratification and drag reduction and additionally trap sediment (Zhu et al., 2021a; Zhu et al., 2022). In addition, groins constructed alongside the navigation channel have captured large amount of sediment due to sheltering effects which can contribute to the siltation due to channel-to-shoal and shoal-to-channel sediment exchange (Zhou et al., 2021). The effect of two long jetties on hydrodynamics have been studied; for instance, they increase the friction and therefore enhance tidal damping (Zhu et al., 2021b); and intensify the landward residual in the South Passage and therefore increase the salinity (Wu et al., 2010). The two long jetties also play a role in the erosion of the subaqueous delta, and the eroded

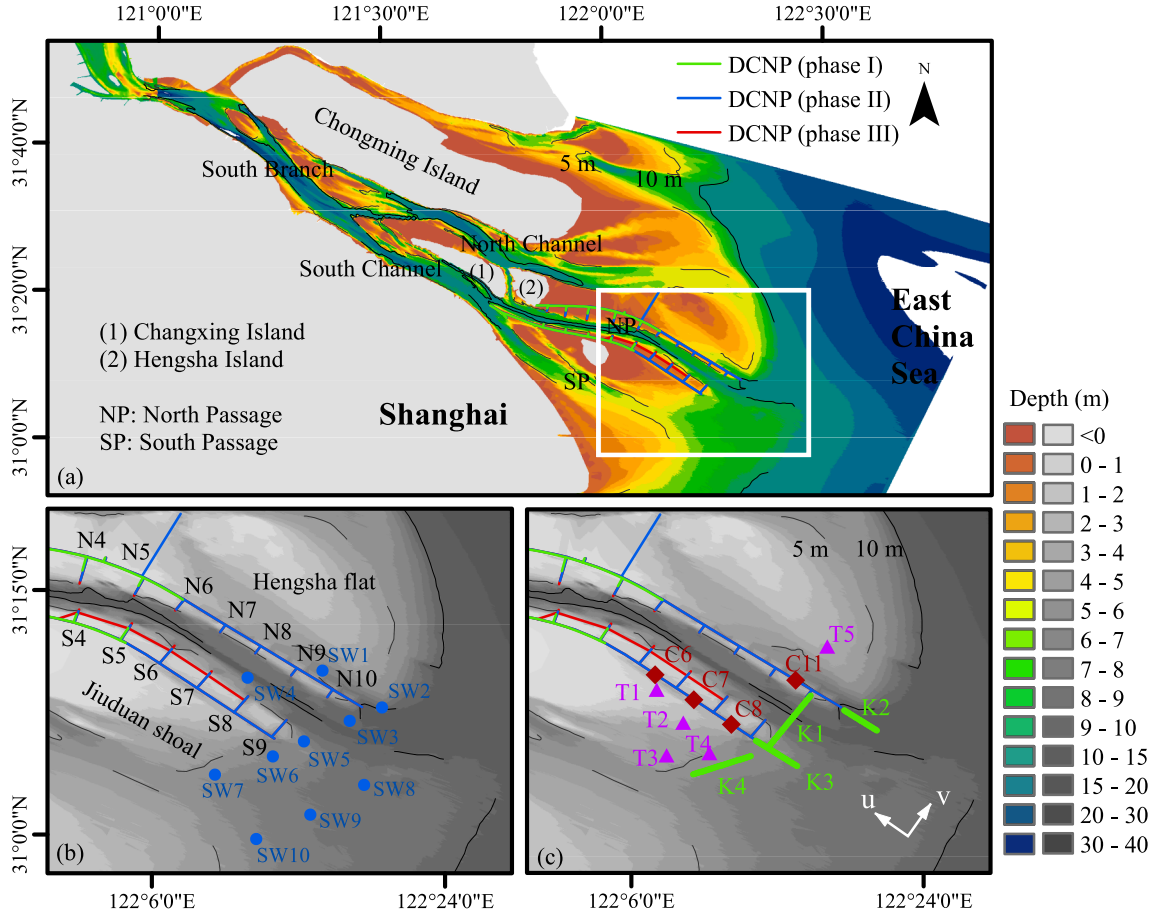

Fig. 1. Study area of the Yangtze Estuary (a), the locations of (b) SW1-SW10, and (c) C6, C7, C8, C11 on the jetties, T1-T5 on the tidal flats, and the transects K1-K4 for the field measurement in 2014. N4 – N10 and S4 – S9 in panel (b) are groin numbers to indicate the modifications of the sediment barrier (in red) in Table 2. (For interpretation of the references to colour in this figure legend, the reader is referred to the web version of this article.)

sediment provides an important sediment source to the main channel (Zhu et al., 2016). The lateral sediment transport between the North Passage and the channels to its South and North is partially blocked by the jetty. Nevertheless, water and sediment transport over the jetty could still constitute an important sediment flux potentially providing an additional sediment source for siltation in the North Passage. But despite their potentially large impact, the amount of water and sediment exchanged over these jetties as well as the mechanisms driving this exchange remain unexplored in scientific literature.

In this study, we collected in-situ data in the channel-shoal system of the Yangtze River mouth in the dry and wet season in 2014. We aim to explore the horizonal sediment exchanges in the distributary system disturbed by local structures in the Yangtze Estuary, especially quantifying the over-jetty water and sediment exchanges. The paper is organized as follows. Section 2 introduces the study area and methods including the field observation and numerical model. Section 3 presents the main results of observations and simulations, focusing on the horizontal circulation and the mechanisms. Section 4 discusses the mechanisms and implications. Section 5 summarizes the main findings.

2. Data and methods

2.1. Study area

The Yangtze Estuary is characterized by three subsequent bifurcations, resulting in four outlets into the East China Sea. The first bifurcates the Yangtze River into the North and South Branch, the second bifurcates the South Branch into the North and South Channel, and the third bifurcates the South Channel into the North and South Passage (Fig. 1). The river discharge is high (monthly averaged value varying between 10,000–80,000 m^3/s) at the tidal limit (Datong station), 640 km upstream of the mouth. Fluvial sediment supply is the main sediment source to the delta, with an annual mean sediment load decreasing approximately 70 % from 425 Mt (1951–2002) to 129 Mt (2003–2022). It has been estimated that 40–60 % of the sediment load used to deposit in the estuary (Milliman et al., 1985). The Yangtze Estuary is a partially mixed mesotidal estuary with a mean tidal range of 2.6 m at the mouth and spring tidal range up to 5.9 m. It has a predominantly semi-diurnal tidal regime with M_2 as the most important component, followed by S_2, O_1, and K_1. The mouth zone of the Yangtze Estuary encompasses the region of the North Passage, South Passage, and the seaward segment of the North Channel, and is known as the turbidity maximum zone due to locally elevated sediment concentrations (Li and Zhang, 1998; Jiang et al., 2013; Guo et al., 2021).

The North Passage is the main navigation channel, which was deepened and protected in three phases as part of the DCNP. The 350–400 m wide channel was first deepened from 6-7 m to 8.5 m (2002, phase I) then to 10 m (2005, phase II) and finally to 12.5 m (2010, phase III) to accommodate progressively larger ships. The structures with two ~ 50 km long jetties (height of 2 m, approximately 1.3 m below MHW) and 19 groins (height of 0–2 m) were constructed to increase the current velocity through the channel and thereby minimize sediment deposition. In addition, a ~ 20 km sediment barrier near the lower southern jetty was also constructed in the phase III during 2005–2010 but with continuous modifications later (see Table 2 in the discussion). The sediment barrier were constructed at a height of 2.5 m and periodically submerged during high water. Since implementation, an annual dredging volume of ~ 50–60 million m^3 was required to maintain the depth of the North Passage (Zhu et al., 2019). The near-bottom SSC in the North Passage may exceed 10 kg/m^3 and even reach 100 kg/m^3 (Wan et al., 2014; Lin et al., 2021).

2.2. Field observations

In-situ field measurements were carried out in 2014 to understand the water and sediment exchange processes in the channel-shoal system (Fig. 1, Table 1). All data were collected at both spring and neap tides in the dry and wet seasons under calm conditions. In the dry season, the wind speed was mainly < 6 m/s (easterly) and maximum by 12 m with significant wave height of 1–2 m (northerly) at intermediate tide. In the wet season, the significant wave height was < 1.5 m. The field measurements site may be influenced by typhoon, but during the observational period the wind was relatively weak (southerly, mainly 4–5 levels). The river discharge, measured at Datong, were 12,000 ~ 15,000 m^3/s and 45,000 ~ 53,000 m^3/s in the dry and wet season, respectively.

Velocity, salinity, and SSC were hourly measured at 10 stations in the channel (SW1-SW10). Velocity, salinity, and SSC observations were additionally collected every 30 min at four transects (K1 ~ K4), where each transect was measured simultaneously using two boats from two sides to the center with a spacing of 100 m. Velocity was measured by Acoustic Doppler Current Profiler (ADCP, Nortek) looking downward whereas turbidity was measured by Optical Backscattering Sensors (OBS, Campbell). All the samples were collected in six relative-depth layers by moving the instruments from water surface (~0.5 m below the surface, corresponding to $z/H = 0.05$) to 0.2, 0.4, 0.6, 0.8 and 0.95 (near the bed), where H is the water depth, and z denotes the height above the bed. A water sample of 1.2 L was collected at each layer. These water samples were used for laboratory analysis of SSC and salinity to calibrate OBS.

On the tidal flats, velocity was measured at 5 stations (T1-T5) every 30 min by ADCP in six relative-depth layers (same relative vertical position as the channels). To assess near-bed sediment transport, salinity was measured near the surface and 0.5 m above the bed (mab, hereafter) whereas sediment concentrations were measured near the surface, 1.2, 0.5 and 0.25 mab; both covering a spring-neap tidal cycle. The north and south jetties are periodically inundated. To measure the over-jetty flow and sediment transport, 4 sites (C1-C4) were selected on the jetty to measure the water depth, velocity, salinity, and SSC every 30 min.

2.3. Data analysis

The SSC was obtained by calibrating OBS using water samples. In the laboratory, the OBS (turbidity in NTU) was calibrated in a cylindrical container (0.4 m in diameter and 0.5 m in height) with continuous and steady stirring at the bottom. The container was filled with the water collected in the Yangtze Estuary and a mixture of bottom sediment collected every 2 h within a campaign). The OBS was mounted at 15 cm above the bottom with an outlet at the same height for sampling. The mixture was gradually diluted, and at each SSC level, a water sample was taken after the turbidity readings stabilized for 30 s. Subsequently, the water samples were filtered through a pre-weighed filter (0.45 μm), and the filter was dried at 40℃ for 48 h and reweighed to determine the SSC. Averaged turbidity during the sampling was then calibrated against the SSC of water samples.

We calculate the instantaneous sediment flux at near-bed and total

Table 1
Field measurements for sampling sites and periods. SSC: suspended sediment concentration.

Region	Sampling time	Dry stations	period	Wet stations	period
channels	spring	SW1-SW10	Feb. 28-Mar. 1	SW1-SW5, SW8-SW10	July 13–14
	neap	SW1-SW10	Feb. 23–24	SW1-SW5, SW8-SW10	July 20–21
transects	spring	K1-K3	Feb. 28-Mar. 1	K1-K4	July 13–14
	neap	K1-K3	Feb. 23–24	K1-K4	July 20–21
tidal flats	spring-neap cycle	C6-C8, C11, T1-T5	Feb. 23-Mar. 1	C6, C8, C11, T1-T5	July 13–21

water depth to indicate the temporal changes in sediment flux particularly for the over-jetty sediment transport. The residual sediment flux is the averaged sediment flux over a tidal cycle of 25 h to imply the sediment transport pattern and long-term morphological changes. We calculate the terms as follows:

The i^{th} layer (e.g., near-bed) instantaneous sediment flux f_i (kg m^{-1} s^{-1}) is calculated as:

$$f_i = u_i c_i h_i$$

The i^{th} layer (e.g., near-bed) residual along or cross-channel sediment flux F_i (kg m^{-1}) is calculated as:

$$F_i = \int_0^T f_i dt$$

Where u_i is the along or cross-channel velocity at the i^{th} layer. c_i is the sediment concentration at the i^{th} layer; h_i is the depth of the i^{th} layer, and the depths of the layers from the surface to bottom are 0.05H, 0.2H, 0.4H, 0.6H, 0.8H, and 0.95H, respectively (H is the instantaneous total depth) due to the six-layer measurements. T is 25 h for each spring and neap tidal cycle. Therefore, the instantaneous and residual sediment fluxes over total water depth are the sum of the values at each layer.

2.4. Numerical model

The hydrodynamic exchange processes are analyzed in greater detail using a 3D hydrodynamic model. This model is based on validated Delft3D model with 1,173 × 374 orthogonal curvilinear grids from Zhu et al. (2021a, b) but with modified boundary conditions (simulating a spring-neap tidal cycle in 2014 with realistic forcing of river discharge measured at Datong). The numerical method is based on a finite difference scheme solving the 3D Navier-Stokes equations and sediment transport described by the advection–diffusion equation. The seaside water level boundary is prescribed with amplitudes and phases of 12 astronomic tidal constituents (M_2, S_2, N_2, K_2, K_1, O_1, P_1, Q_1, MF, M_4, MS_4, and MN_4) derived from the TPXO 7.2 Global Inverse Tide Model. The model was run in 3D using 10 vertical sigma layers to resolve baroclinic flow dynamics and flow over the jetties and groins in the North Passage as structures partially blocking through- or overflow (instead of completely blocking exchange). Alongshore residual flows resulting from large-scale ocean currents were added as well but since these flows were found to have minor effect on exchange flows, we do not further consider ocean currents. Moreover, the realistic southerly wind forcing is implemented.

The model is calibrated well for the measured water level and velocity in 2014 (see details in Supporting Information, SI). Although the model poorly simulates the salinity on tidal flats, this does not negate out results as it can still capture the over-jetty sediment transport processes between the channel and shoal. Several scenarios were executed to explore the effect of natural forcing and human activities. The reference scenario with partially blocked jetties is calibrated. The following scenarios are implemented with systematically changing one parameter while keeping the others the same as the reference scenario: 1) without Coriolis effect; 2) without wind effects; 3) blocked jetties and groins; 4) without jetties and groins; and 5) with reclamation of the Nanhui flat.

3. Results

3.1. Sediment transport on tidal flats

For each station on the tidal flats, the instantaneous sediment transport rates are of the same order of magnitude in the North-South and the East-West direction (Fig. 2). In the dry season the maximum instantaneous transport rates on Jiuduan shoal (T1-T4, south of the North Passage) range between 0.4 – 0.8 kg/m^2/s; in the wet season the maximum fluxes and the spread is larger (range between 1 and 3 kg/m^2/s). Sediment transport on Hengsha flat (T5, north of the North Passage) is slightly lower (up to 0.2 kg/m^2/s in the dry season and 1.5 kg/m^2/s in the wet season) but also more asymmetric (westward fluxes 4–6 times the eastward fluxes in the wet season).

To better quantify sediment transport from the shoal to the channel, the data is decomposed in an along-channel and cross-channel component (using the grey line in Fig. 2) and converted to a residual flux (Fig. 3). Herein the tidal oscillation indicates the flood-ebb transport while the trend reveals the residual sediment transport. On Jiuduan

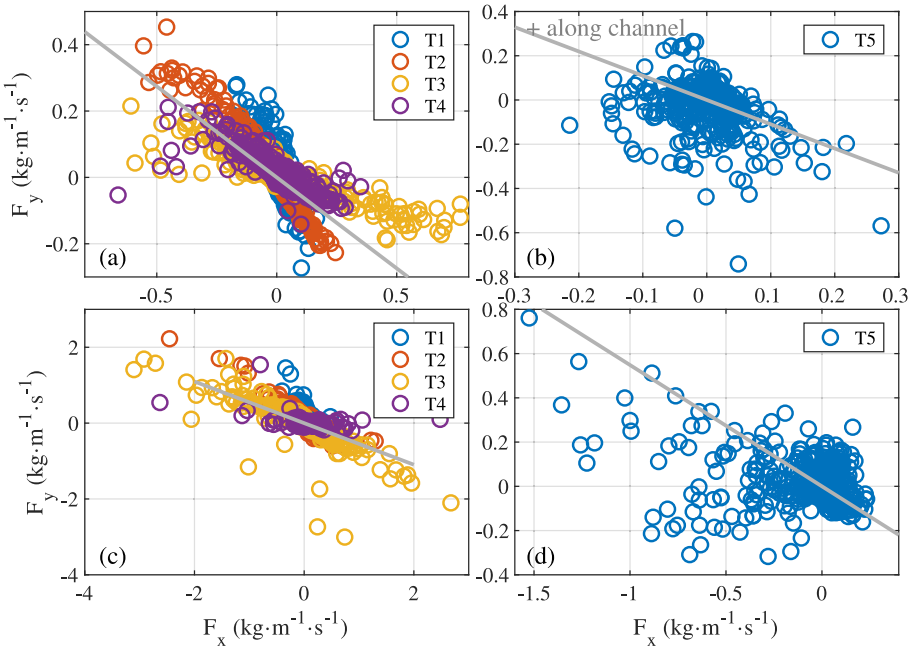

Fig. 2. Relationship between near-bed sediment flux to the East (F_x) and North (F_y) at T1, T2, T3, and T4 (a, c), and at T5 (b, d) in the dry (a, b) and wet season (c, d). 'Near-bed' is herein defined as the velocity in the lowest cell and the sediment concentration measured at 0.5 mab. The grey lines indicate the along-channel direction (used to define along-channel and transverse transport in Fig. 3). Flood currents are in the NW direction, ebb currents in the SE direction.

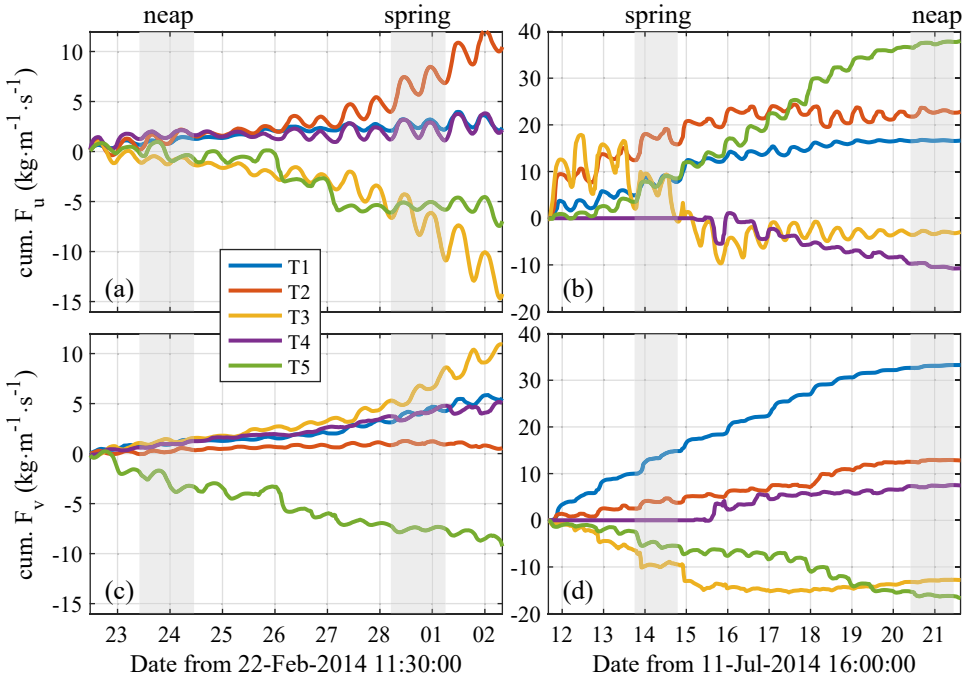

Fig. 3. The changes in cumulative near-bed sediment flux at T1-T5 in the along-channel F_u (a, b) and cross-channel F_v (c, d) direction in the dry (a, c) and wet season (b, d). Note that the horizontal line at T4 in the wet season indicates no data. The shaded grey area are the spring and neap tide periods of data collection at locations C6, C8, C11.

shoal, the largest along-channel sediment import is at T2 (both dry and wet season) and T1 (especially wet season); along-channel sediment export is only observed at T3 in the dry season but also at T4 in the wet season. In the lateral direction (cross-channel) on Jiuduan shoal, the residual sediment transport is typically towards the North Passage, except for station T3 during the wet season. Interestingly, T3 also has the largest lateral sediment flux towards the North Passage in the wet season. This suggests significant lateral water and sediment exchanges at T3 on a seasonal scale. On Hengsha flat (T5), the along-channel residual sediment transport is in the seaward direction in the dry season and in the landward direction in the wet season, suggesting significant longitudinal sediment exchanges. The lateral sediment fluxes are negative in both dry and wet seasons implying persistent southward sediment transport from the Hengsha flat. However, this lateral sediment

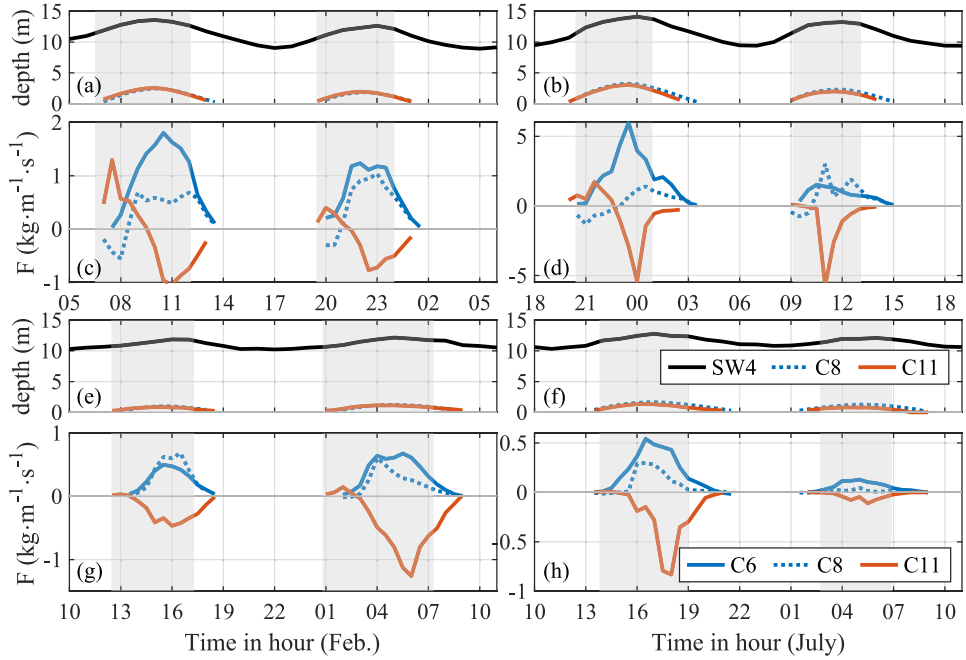

Fig. 4. Changes in water depth at SW4, C8 and C11 (a, b, e, f) and the unit width cross-channel sediment flux at C6, C8, and C11 (c, d, g, h) at spring (a, b) and neap (c, d) tide in the dry (a, c) and wet (b, d) season. The shaded grey indicates the flood period detected from the depth-averaged along-channel velocity at SW4. Positive cross-channel sediment flux indicates that sediment transports towards the North Passage, i.e., from Jiuduan shoal to the channel (C6, C8) and from the Hengsha flat to the channel (C11).

transport mainly contributes to the development of the southern Hengsha flat rather than to siltation in the North Passage because flow and sediment transport over the jetty (at location C11) is directed northward (as described later).

3.2. Over-jetty sediment transport

As the jetties are partially blocked, water carrying suspended sediments can flow over the jetties at high water, influencing exchange of water and sediments between channel and shoals (Fig. 4). The jetties are submerged on averaged 6 h per tidal cycle with the minimum by 3.5 h and the maximum by 8 h, covering 36–60 % of the total time. Sediment exchange between the southern bank (Jiuduan shoal) and the North Passage is largely towards the channel. Sediment transport from the channel to the shoal only occurs at C8 at the early flood of spring tide, lasting 1–3 h. Sediment is transported from the shoal to the channel on all other time periods (C8) and locations (C6, C7). The residual sediment flux is also larger at C6 (25.5, 9.8, 51, and 5.4 Mt/m tide in the spring and neap of the dry and wet season, respectively) than that at C8 (13.9, 8.1, 22, and 2.4 Mt/m). The sediment flux is more strongly related to the sediment availability than to the period of overflow. For instance, the over jetty-flow at C6 and C8 lasts shorter at spring tide than neap tide both in the dry and wet season, but the resulting transported flux is the larger because of the highest sediment concentration. In addition, the over-jetty flow starts ~ 1 h later than the beginning of the flood and stops ~ 1 h later than the beginning of the ebb due to the distance between C8, C6 and SW4.

Sediment transport is mostly from channel to shoal on the north bank. Sediment is only transported from Hengsha flat to the North Passage at the early flood of spring tide. But most of the time, sediment is transported from the North Passage to Hengsha flat with residual sediment fluxes of 10.3, 12.4, 29, and 4.6 Mt/m at spring and neap tide in the dry season and wet season, respectively.

3.3. Residual sediment fluxes

The residual sediment fluxes in the channels and on the shoals at different periods are illustrated in Fig. 5. Especially the fluxes over the jetties reveal a strikingly persistent northward transport (both the northern and southern jetty). The fluxes over Jiuduan shoal display a clockwise circulation pattern, transporting sediment landward from the East China Sea onto Jiuduan shoal (and which is subsequently transported into the North Passage). The observations close to the North Passage reveal a seaward directed flow during spring tides while neap tide transport is landward (in both season). This may be related to spring-neap variations in mixing and the near-bed position of the observations. During spring tides, the water column is completely mixed and as a result the residual flow resulting from the freshwater discharge of the Yangtze River drives a residual seaward sediment flux (which is therefore larger during the wet season). During neap tides the water column is stratified and a landward flow close to the bed drives a residual landward sediment flux.

The transect observations in deeper water confirm the clockwise circulation between Jiuduan shoal and North Passage. In addition, this circulation is especially strong at spring tides when the residual flux in the main channel is seaward. When the residual flux in the channel is landward (neap tides), this circulation is weaker either by southward residual transport near the southern jetty in the channel (Fig. 5d) or by depth-averaged seaward sediment transport (Fig. 5h). Note that although the residual sediment flux is landward near the bed (see Fig. 5g), the depth-averaged residual sediment transport is often seaward (Fig. 5h) because of seaward directed residual flows higher in the water column. A weaker circulation cell is observed at the northern jetty with offshore sediment transport into the channel and then towards Hengsha flat. Moreover, sediment transport from the channel to the Jiuduan shoal at transect K3 (yellow arrows) also indicates a weak anticlockwise sediment transport from the Jiuduan shoal to the southern groin field (see Fig. 5b).

3.4. Large-scale hydrodynamics

The analysis of field observations reveals a very pronounced south-to north residual transport component. The mechanisms responsible for this residual flow are further explored using a well-calibrated hydrodynamic model resolving barotropic and baroclinic flows. This model clearly reveals the existence of a pronounced water level difference between Jiuduan shoal and the North Passage, and between Hengsha flat and the North Passage (Fig. 6). This is supported by observed water levels, with the M_2 tidal amplitude in the middle of the South Passage being approximately 0.07 m larger than that in the middle of the North Passage (Fig. 6a). Such a water level differences drives a northward-directed barotropic flow at high water, likely enhancing sediment transport from the South Passage to the North Passage. The phase of the main constituent M_2 is ~ 324 ° in the middle of the South and North Passages, respectively (Fig. 6b) so the water level gradient is the result of tidal amplification differences rather than propagation speed. Moreover, significant water level differences also occur between the Jiuduan Shoal and North Passage, and between North Passage and Hengsha flat. During both the end of flood and beginning of flood, the computed water level on the Jiuduan shoal near the southern jetty is higher than in the North Passage, suggesting over-jetty flow and sediment transport from Jiuduan shoal and Hengsha flat to the North Passage (Fig. 6c, d). Similarly, the tidal water level is higher in the North Passage than over Hengsha flat, leading to the over-jetty water and sediment transport from the North Passage to the Hengsha flat.

To better understand the mechanisms driving the large-scale water level gradient, we conduct several numerical experiments on physical processes driving the flow as well as human interventions that may have strengthened the cross-channel flow. We evaluate these experiments in a Lagrangian framework using numerical tracers released at two sites on the Jiuduan shoal and Hengsha flat. We subsequently investigate the effects of two physical parameters (Coriolis and wind) and two human interventions (the DCNP and reclamation in the channel-shoal system south of the South Passage) – see Fig. 8.

The jetties and groins strongly influence sediment exchange patterns while other effects play a limited role. For instance, the reference case suggests over-jetty flows and circulations between the shoal and the North Passage which is consistent with our observations (Fig. 8a). When flow and transport over the jetties is blocked (Fig. 8c), sediment is mainly exchanged between Jiuduan shoal and Hengsha flat seaward of the jetty. Additionally, Hengsha flat becomes an important sediment source for the North Passage, passing the seaward extent of the northern jetty. Removing the constructions (Fig. 8d), Hengsha flat is highly dynamic with circulations covering the whole tidal flat whereas the sediment on the Jiuduan shoal strongly exchanges with the South Passage. This may promote higher siltation in the South Passage and on Hengsha flat compared to the reference case. Another major human intervention in the Yangtze Estuary mouth (reclamation of Nanhui flat along the south bank of the South Passage) appears to have a minor impact on sediment exchange. Also wind-driven flow has a much smaller impact on water exchange compared to the scenarios with full, partial or no flow over the jetties. The Coriolis effect is very important – this will be discussed in greater detail in the following section.

4. Discussion

4.1. Sediment budget

Understanding a system's sediment budget is essential for predicting the effect of changing water and sediment dynamics on its morphology and ecology. Previous studies in the Yangtze have unraveled the sediment flux a larger scale (Xie et al., 2017b; Guo et al., 2021) or focused on

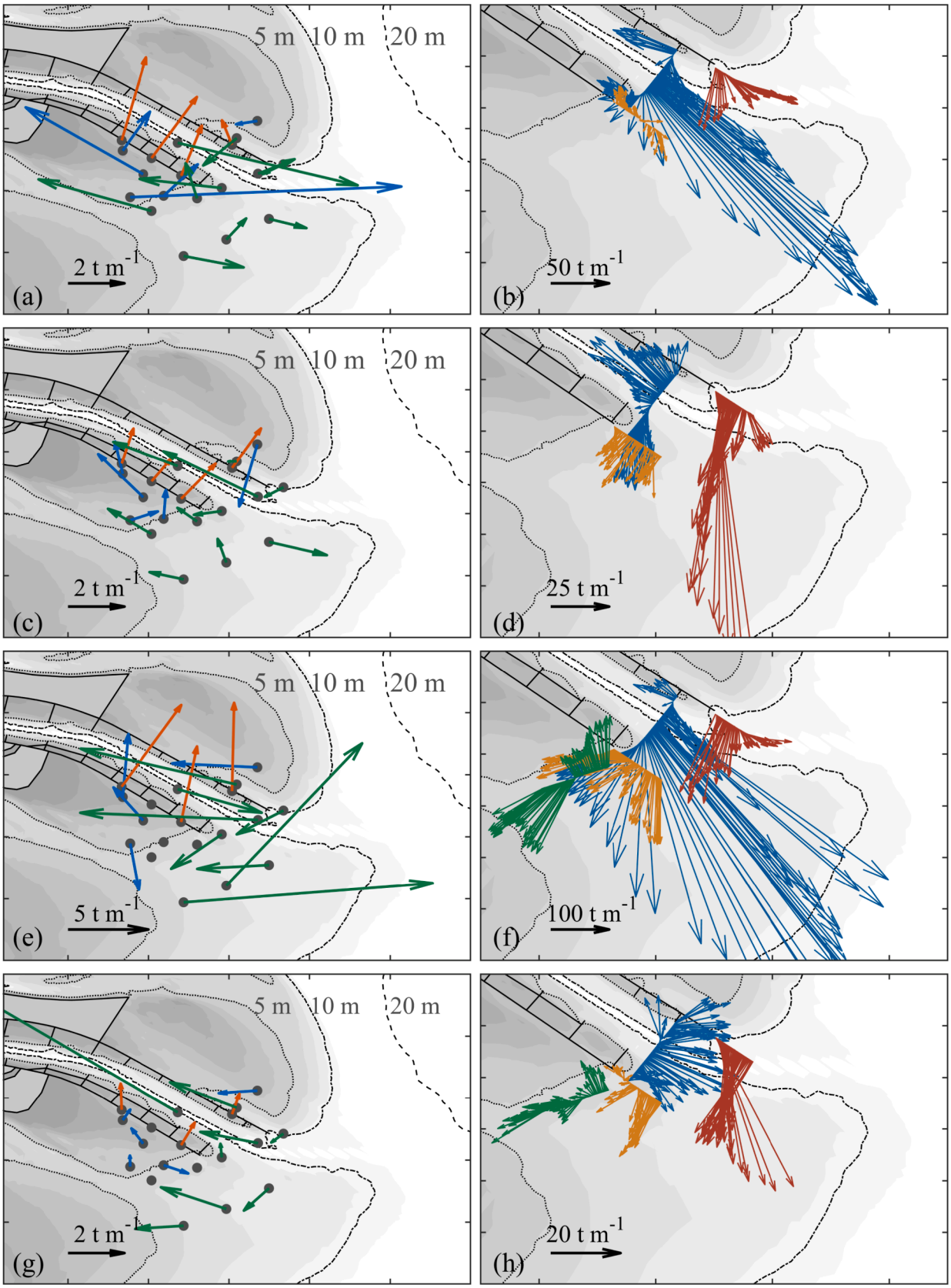

Fig. 5. The unit width residual sediment fluxes over a 25-hour tidal cycle (tonnes/m) at (a, b, e, f) spring and (c, d, g, h) neap tide during (a-d) dry and (e-h) wet season. The residual sediment fluxes are near bed at (a, c, e, g) stations and over the water column at (b, d, f, h) transects. Transport fluxes of the SW stations are green vectors; T stations are blue vectors, and C stations are red vectors (a, c, e, g). Transect K1 is depicted in blue arrows; K2 in red arrows; K3 in yellow arrows and K4 in green colors (b, d, f, h). (For interpretation of the references to colour in this figure legend, the reader is referred to the web version of this article.)

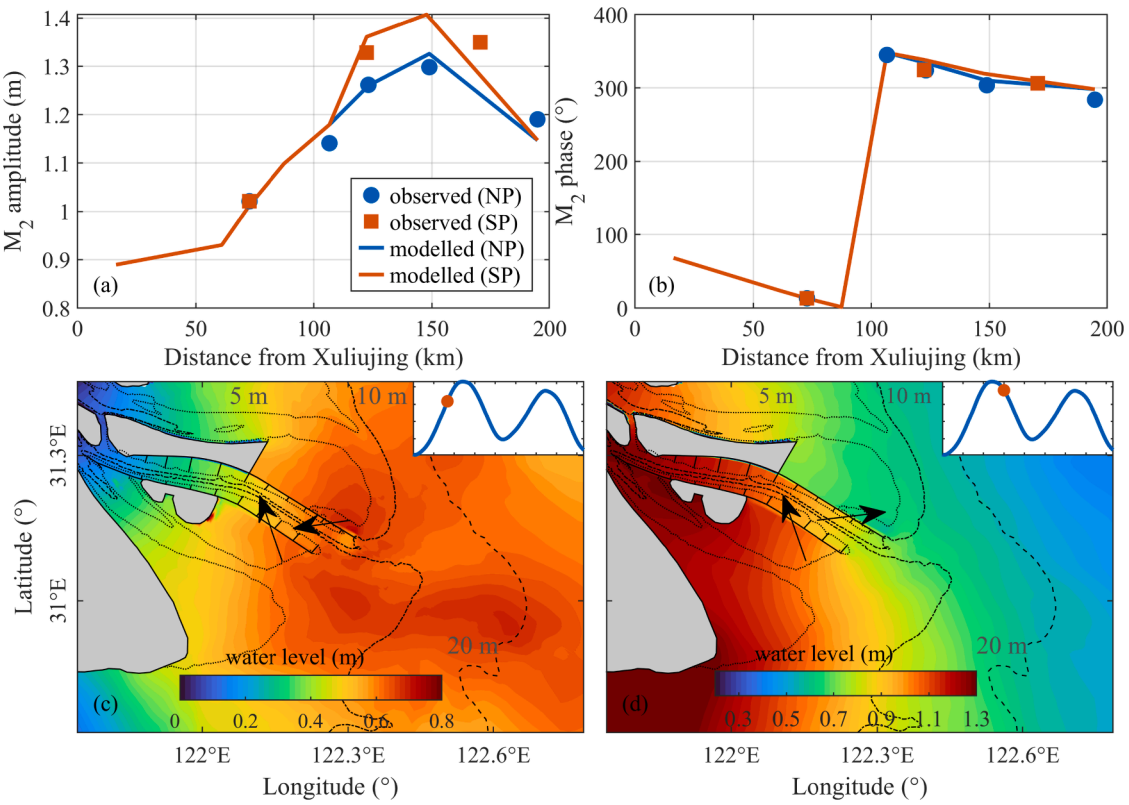

Fig. 6. The observed modelled M_2 amplitude (a) and phase at stations along the North Passage (NP) and South Passage (SP) in July 2014. The spatial variations of water levels at the specified rising time and falling time indicated by the red dots of the time series of the water levels at SW4 (see Fig. 1 for the location). (For interpretation of the references to colour in this figure legend, the reader is referred to the web version of this article.)

other regions such as the South Passage (Zhang et al., 2022; Wang et al., 2024). Here, we focus on the North Passage in the mouth zone, the main navigation channel of the Yangtze Delta. Based on in-situ data in the region among the Jiuduan shoal, Hengsha flat, North Passage and its seaward area, we identify the sediment budget in terms of suspended sediment flux, illustrating how sediment is exchanged between the main outflow channel, the channel-shoal system, and the East China Sea (Fig. 7). Regardless of the wet and dry season, the largest flux is through the North Passage, particularly at spring tide. The over-jetty sediment transport is directed northward from Jiuduan shoal towards the channel, and from the channel towards the Hengsha flat. However, in the dry season and during neap tides, a clockwise circulation occurred at neap tide at the tip of the northern jetty where sediment is transported northward from the channel onto Hengsha flat, further seaward the sediment is transported back southward from Hengsha flat into the channel, and subsequently landward. The clockwise circulation in the wet season at the tip of southern jetty is larger, providing a mechanism through which sediment exported from the North Passage flows back into the channel via Jiuduan Shoal. This could therefore provide a previously unknown mechanism contributing to sediment trapping in

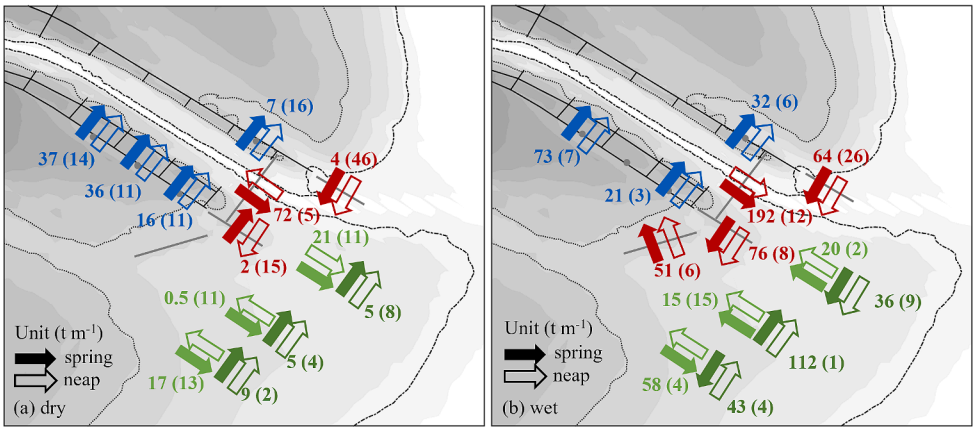

Fig. 7. Sediment budget showing the depth-averaged residual sediment fluxes computed over a 25-hour tidal cycle during the (a) dry and (b) wet season. The approximate direction of transport is provided for spring (filled arrow) and neap (non-filled arrow) conditions; the magnitude of the flux is provided with the numbers (with the neap tide flux in brackets). Transport fluxes at SW8, SW9, SW10 are indicated by light green (along-channel) and dark green (cross-channel or lateral) arrows; Transects and C stations are depicted only for the component perpendicular to the section in red and blue arrows, respectively. (For interpretation of the references to colour in this figure legend, the reader is referred to the web version of this article.)

the navigation channel. This northward flux is supplemented with sediment transported seaward in the South Passage, as was suggested by previous studies (Zhang et al., 2022; Zhu et al., 2024), strengthening the clockwise sediment pathways. Therefore, the two long jetties act in different ways redistributing sediment: the northern one diverts sediment from the channel and Hengsha flat away whereas the southern one recycles sediment between Jiuduan shoal and the channel. Moreover, the seasonal changes indicate that sediment trapping in the wet season is more pronounced than that in the dry season. This wet season trapping is consistent with previous findings although the density-driven flow and tidal asymmetry are often regarded as one of the main reasons (e.g., Jiang et al., 2013; Wan et al., 2014). Note that although the sediment budget relies on the year-2014, it is representative as the river and tidal forcing as well as sediment load are normal in 15 years (2006–2021) which exclude extreme conditions.

4.2. Sediment transport mechanisms

4.2.1. Horizontal water level gradient

The horizontal water level gradients play an important role in sediment transport, particularly for lateral sediment exchanges. The tidal amplitude is overall higher in the South Passage than the North Passage (see also Lu et al., 2015; Alebregtse and de Swart, 2016). This horizontal water level gradient generates northward over-jetty sediment transport from Jiuduan shoal towards the North Passage and from the North Passage to the Hengsha flat around high water, especially during the flood period (see Fig. 4 and Fig. 6). Note that the sediment exchange between the North Passage and Hengsha flat is towards the channel in the early flood and towards the shoals in late flood and early ebb. This is mainly caused by the clockwise rotation tidal systems in the mouth of the Yangtze Estuary where the semi-diurnal tidal current transports water southward at maximum ebb and northward following maximum flood (Larsen et al., 1985; Byun and Hart, 2022). Moreover, due to the interaction between the tide and the shallow water depth, Stokes transport drives a residual circulation which results in most salt intrusion in the South Passage and most river runoff discharging through the North Channel (Wu et al., 2010).

Estuarine water levels are influenced by astronomical tides, river flow, bathymetry, as well as coastal processes such as the Coriolis effect, wind, and reclamation explored in this study (see Fig. 8). The Coriolis effect is hypothesized as one of the major forces driving the southward sediment transport in the river mouth through its influence on tidal flow processes (Li et al., 2011). Our simulation confirms its apparent important role in the southward sediment transport seaward of the

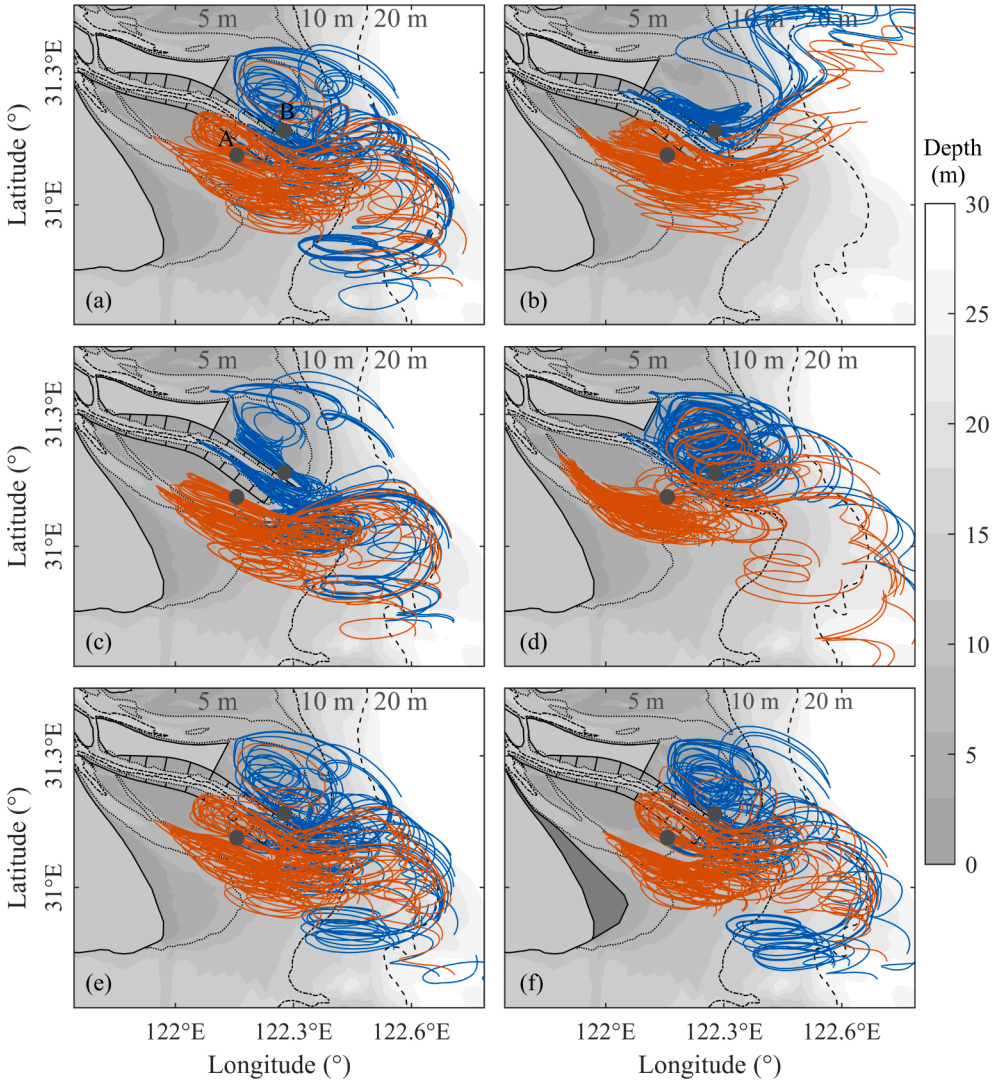

Fig. 8. The sediment transport paths of the tracers on the Jiuduan shoal (A, in red) and Hengsha flat (B, in blue) over 25 h at spring tide in the wet season in scenarios (a) reference, (b) no Coriolis effect, (c) jetties with blocking effects, (d) no jetties and groins, (e) without wind effects, and (f) reclaimed Nanhui flat (in dark grey). (For interpretation of the references to colour in this figure legend, the reader is referred to the web version of this article.)

Yangtze Estuary. Another (but smaller) effect of Coriolis is that it decreases the landward sediment transport into the North Passage, which is consistent with earlier work by (Gong et al., 2021). Wind is typically expected to affect sediment transport directions, especially in the surface whereas land reclamation could reduce tidal prism which may lead to shifts in sediment import and export (Wu et al., 2010; Guo et al., 2022; Seo et al., 2023; van Maren et al., 2023b). However, this study indicates a limited role of both.

4.2.2. Flow and tidal asymmetry

Residual transport of sediment often results from an asymmetry in the flow. This flow asymmetry may in turn be generated by tidal asymmetry and by residual flow. Tidal asymmetry is an important driver of residual transport in any estuaries (Speer and Aubrey, 1985; Wang et al., 2002; Song et al., 2013; Zhang et al., 2018). A method to quantify the degree of tidal asymmetry and can be applied to relatively short timeseries such as ours is the third moment about zero, normalized by the second moment about zero to the 3/2 power (Nidzieko and Ralston, 2012):

$$\gamma_0 = \frac{\mu_3}{\mu_2^{3/2}}$$

Whereas the m-th moment about zero is defined as:

$$\mu_m = \frac{1}{N-1}\sum_{i=1}^{N}(n_i)^m$$

And N is the number of samples n_i. Here we calculate the along-channel and cross-channel velocity asymmetry in the dry and wet seasons. We define the flow asymmetry as the skewness of the total observed flow velocity while we define tidal asymmetry as the asymmetry in the velocity signal of which the residual component has been removed using a Godin filter (Walters and Heston, 1982). In other words, the flow asymmetry is the combined effects of residual flow (due to river-tide interaction) and tidal asymmetry (due to tidal deformation).

The changes in velocity skewness in the dry and wet season indicate the effect of tidal and/or flow asymmetry (Fig. 9) on the net sediment transport (see Fig. 3). In the along-channel direction, the net landward sediment transport at T1 and T2 in both the dry and wet season is caused by the flood-dominant flow induced by both the tidal and flow asymmetry, both having positive velocity skewness. The flow asymmetry on positive velocity skewness is larger than tidal asymmetry, which suggests a larger contribution of flow asymmetry on the net landward sediment transport at T1 and T2. At T3, the net seaward sediment transport in both the dry and wet season results in negative total velocity skewness whereas velocity skewness due to tidal asymmetry is positive. This suggests that residual flow due to river-tide interaction rather than tidal asymmetry controls the net seaward sediment transport, highlighting the important role of river discharge. Similarly, at T4, the net seaward sediment transport in the wet season is mainly ascribed to residual flow. However, the net landward sediment transport in the dry season is caused by both tidal and flow asymmetry. The different changes in net sediment transport and the asymmetry in the dry season between T3 and T4 are closely related to the location. Specifically, T3 is located near the main channel of the South Passage whereas T4 is located in the tidal channel on the tidal flat, leading to the stronger and weaker interactions between river and tides at T3 and T4, respectively. In contrast, at T5, net seaward and landward sediment transport is observed in the dry and wet season, respectively, with the seaward transport in the dry season mainly driven by residual flow. The latter indicates the important role of flow asymmetry rather than tidal asymmetry as the residual effect weakened the ebb-dominance.

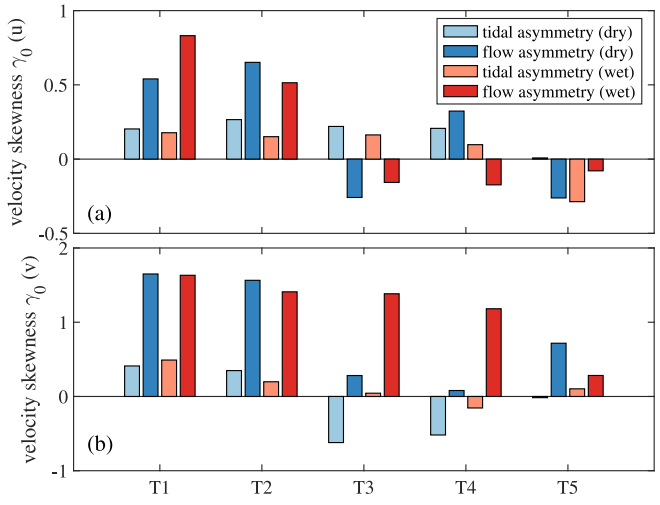

Fig. 9. Vertical distribution of the along-channel (a) and cross-channel (b) current velocity skewness in the dry (in blue) and wet (in red) season. Positive along-channel skewness indicates landward net sediment transport whereas positive cross-channel skewness indicates net sediment transport towards the channel. Note that the sign of the cross-channel velocity at T5 is reversed to indicate the towards-channel velocity in the lateral direction. (For interpretation of the references to colour in this figure legend, the reader is referred to the web version of this article.)

In the cross-channel direction, the net sediment transport is overall towards the channel at all sites on tidal flats (Fig. 3). Fig. 9b shows that this transport towards the channel is controlled by flow asymmetry (high positive velocity skew) rather than tidal asymmetry (low velocity skew, and sometimes negative). The exception is at T5 where tidal asymmetry controls the net sediment transport towards the channel. Note that the net sediment transport at T3 is slightly towards the shoal at spring tide in the wet season, which suggests that tidal asymmetry should also not be neglected therein.

Overall, the residual flow due to the river-tide interaction dominates net sediment transport on tidal flats both in the longitudinal and lateral direction whereas tidal asymmetry plays a weaker role mainly at T1 and T2 (dry and wet season), T3 (wet season), and T4 (dry season), but dominates the lateral sediment transport at T5.

4.3. Implications for channel siltation and delta evolution

The DCNP is constructed during 1998–2010 within three phases stepwise increasing the water depth; however, the structures influencing the water and sediment exchanges are continuously modified (Table 2). During the construction works, the sediment concentration in the Yangtze river is reduced by sediment trapping in upstream dams (notably the Three Gorges Dam). The sediment concentration at the tidal

Table 2
Channel deepening and interventions in the North Passage. Jetties are herein defined as along-channel structures and groins as structures perpendicular to the main river flow. The depth and the elevations of the structures are based on local Wusong datum which is approximately 3.3 m below MHW in the North Passage (Fu, 2013).

Year	Interventions
1998–2002 (phase I)	Construction of jetties (2 m) and groins (0–2 m) in the upper North Passage; deepened to 8 *m*
2002–2005 (phase II)	Construction of jetties (2 m) and groins (0–2 m) in the lower North Passage; deepened to 10 m, lengthened groins
2005–2010 (phase III)	Construction of a sediment barrier (2.5 m) at S3.5-S8 (21.2 km, see Fig. 1), deepened to 12.5 m, lengthened groins
2015–2016	Construction of sediment barrier at S8-S9 (19.22 km), elevated the sediment barrier at S4-S9 (4.6 km) to 3.5 *m*
2019–2020	Elevated the sediment barrier at S3.5-S9 (24.8 km) to 4.5 *m*
2023-	Elevated the lower northern jetty to 6 m in the western part (18.364 km), 4–6 m in the transition part (1 km) and 4 m in the eastern part (6.663 km)

limit (Datong station) reduced by 65 % from 1997 to 2007 followed by a slight decrease of 30 % during 2007–2022 (Fig. 10a). Meanwhile, the siltation (based on dredging volumes) in the North Passage increased from 2004 to 2012 and decreased during 2012–2016 and subsequently maintains a relatively constant (and lower) level (Fig. 10b). The poor correlation between the riverine sediment supply and the siltation in the North Passage suggests the important role of the DCNP in trapping sediment. Apart from the trapping mechanisms in the channel which were extensively studied (e.g., Liu et al., 2011; Song et al., 2013; Li et al., 2016; Zhu et al., 2016; Li et al., 2018; Chen et al., 2020; Zhou et al., 2021; Lin et al., 2021; Zhu et al., 2021), this study investigates the contribution of sediment transport over the jetties revealing a clockwise circulating transport cell in the lower channel. Sediment is transported out of the North Passage towards the northern Hengsha flat and towards the channel from southern Jiuduan shoal (see Fig. 4 and Fig. 5).

Taking the Jiuduan shoal- North Passage −Hengsha flat as a channel-shoal system, the siltation in the North Passage and the development of the two shoals are coherently linked due to the sediment transport circulations. Specifically, with the construction of the DCNP phase II, the lower Hengsha flat sustained stronger accretion than lower Jiuduan shoal until 2010, with the accretion rate of 30 $Mm^3\ yr^{-1}$ and 11 $Mm^3\ yr^{-1}$, respectively (Fig. 10c). After a relatively stable development during 2010–2016, the lower Hengsha flat experienced erosion of 16 $Mm^3\ yr^{-1}$ whereas the lower Jiuduan shoal sustained accretion by 7 $Mm^3\ yr^{-1}$. On the other hand, both the northern and southern groins in the lower North Passage experienced sedimentation from 2002 to 2007 (Fig. 10d). Afterwards, the northern groins continued to erode whereas the southern groins showed erosion from 2007 to 2013 and then sustained accretion by 7 $Mm^3\ yr^{-1}$ after 2013. This leads to the smaller channel volume (or more sedimentation) in the southern than norther groins in 2016.

Accordingly, a significant change in the sediment sources and channel-shoal system development can be detected before and after the transition period of 2010–2016 (Fig. 11). During 2002–2010 ('Stage 1'), the Hengsha flat acted as a sediment sink with a significant growth whereas the Jiuduan shoal acted as a sediment source supplying sediment to the channel. In this stage, although riverine sediment supply at Datong is strongly reduced, the sediment supply is still large within the mouth zone (Fig. 10a) because the sediment reduction in the mouth lags the upstream reduction through a morphological response time lag (Zhu et al., 2019) and thus provide sediment to the Hengsha flat. This sediment supply is mainly transported from offshore due to the stronger circulation induced by deepening (Liu et al., 2011; Lin et al., 2021), the resuspension and lateral sediment transport (Chen et al., 2020; Jiang et al., 2013; Zhou et al., 2021) as well as the over-jetty sediment exchange between Jiuduan shoal and North Passage. However, as a sediment barrier was constructed during 2005–2010, the sediment exchange between Jiuduan shoal and North Passage was weakened. Correspondingly, the southern groins reverted from erosion to sedimentation whereas the Jiuduan shoal changed from accretion to erosion in 2007. In the transition period of 2010–2016 ('Stage 2'), the sediment supply within the mouth zone becomes insufficient. The Hengsha flat changed from a sediment sink to a source (erosion) while the Jiuduan shoal remained a sediment source; also the areas around the southern and northern groins started to erode. The adjustment in the channel-shoal system maintained a high channel siltation which peaked in 2012 and the sediment concentration in the North Passage increased. However, the high siltation cannot be sustained longer as observed decreasing siltation in the North Passage after 2012 (Fig. 10a) due to the decreasing upstream riverine sediment supply and the weakened sediment exchange between Jiuduan shoal and North Passage (resulting from the increasingly higher jetties and sediment barriers). However, after 2016 the siltation rates remained constant as by this time the blockage of sediment exchange was nearly complete, which accelerated the development of the Jiuduan shoal ('Stage 3'). In this stage, both the sediment in the North Passage and on the Hengsha flat are sediment sources to promote the growth of the Jiuduan shoal via the clockwise circulation at the mouth feeding Jiuduan shoal, but also with transport from Jiuduan shoal to the North Passage being blocked. This accretion on Jiuduan shoal effectively leads to a southward growth of the delta, strengthening the historical tendency of the seaward prograding of the south bank (Chen et al., 1985). In the future, with further elevated sediment barrier in 2019 and elevated northern jetty in 2023, the sediment exchange in the channel-shoal may be fully blocked and the southward growth of the delta is likely further strengthened.

In the Yangtze Estuary, the trend of southward development is not only strengthened by the DCNP but also other human interventions. A typical example is the shrinkage of the North Branch by land

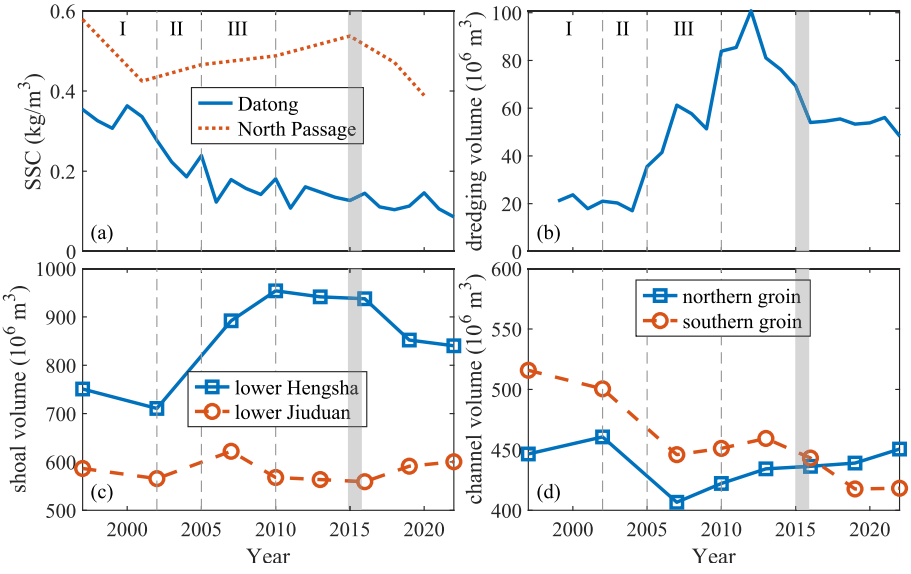

Fig. 10. Changes in (a) suspended sediment concentration (SSC) at Datong and the surface SSC in the North Passage, (b) dredging volume in the North Passage, (c) shoal volume of the lower Hengsha flat and Jiuduan shoal, (d) channel volume at northern and southern groin field during 1997–2022. The sites in the NP and regions are shown in Fig. 11. The dashed lines indicate the phases of the DCNP whereas the shading area indicates that the sediment exchange between Hengsha flat and North Passage was blocked. The dashed grey line indicates the three phases of the DCNP and the thick grey line indicates the time when the sediment barrier is elevated to block the exchange.

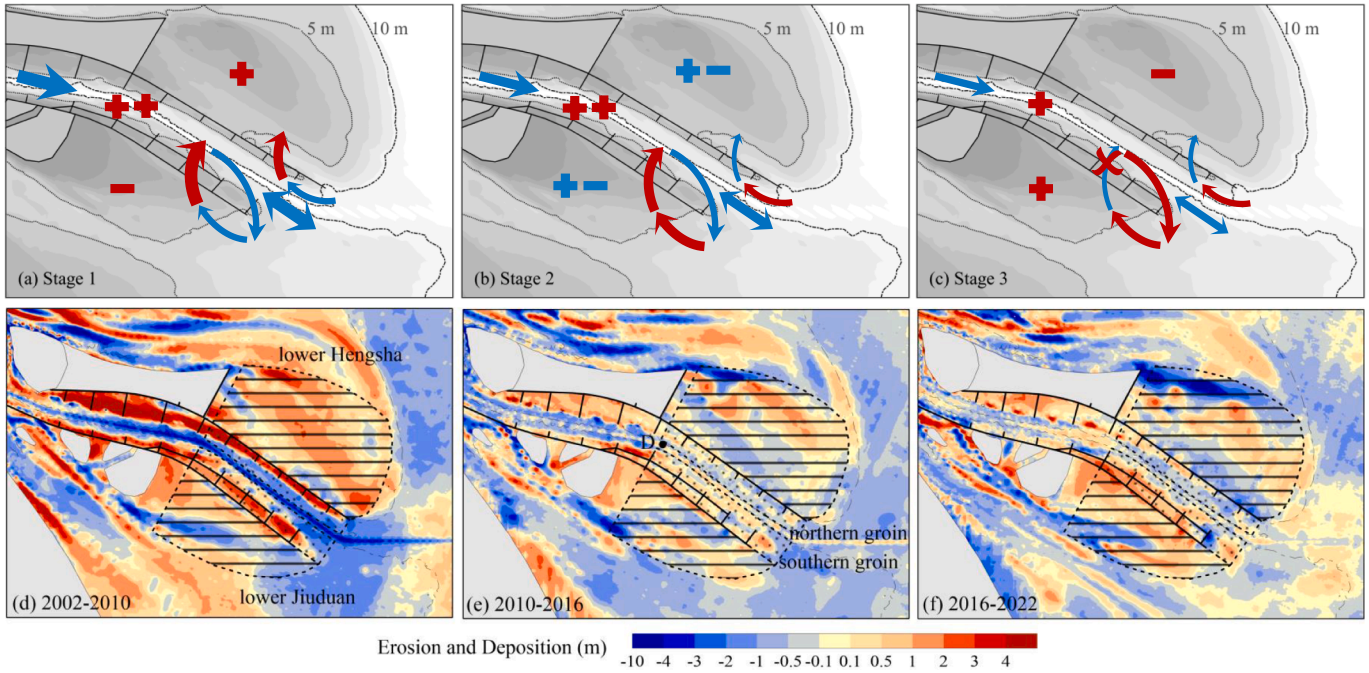

Fig. 11. Schematic sediment transport patterns of (a) Stage 1: strengthened northward growth, (b) Stage 2: transition, (c) Stage 3: strengthened southward growth corresponding to the morphological development of the channel-shoal system during (d) 2002–2010, (e) 2010–2016, (f) 2016–2022, respectively. The marked regions are the volumes calculated in the lower Hengsha flat, lower Jiuduan shoal, northern and southern groins in Fig. 10. The site D is the surface sediment centration in the North Passage from Luo et al. (2022).

reclamation which promote the development of the South Branch in the first bifurcation (Guo et al., 2022). In the second bifurcation, the construction of Qingcaosha Reservoir also reduces the channel volume in the North Channel and promotes the development of the South Channel. Subsequently, the DCNP interferes with the third branch and enhances the growth of Jiuduan shoal as shown in this study. Such an asymmetric development is common in distributary delta systems which is stable to perturbations (Edmonds and Slingerland, 2008), particularly in response to human interventions as the Yangtze Estuary. For instance, a critical level for dumping was identified above which a channel system in equilibrium may become unstable and degenerate in western Scheldt estuary (Jeuken and Wang, 2010). In addition, the asymmetric pattern reflects the combinations of controls including discharge partitioning, lobe abandonment and localized transgression, plume deflection by coastal currents, dominance of longshore current direction, variable subsidence, and other factors (Kakani, 2006; Korus and Fielding, 2015). Thus, the effect of the DCNP on water and sediment exchange and then the southward growth trend is essential to understand the equilibrium state and long-term development of large-scale systems.

We are increasingly realizing how complex but short-term morphological cycles and circulations (such as discussed in this paper) influence the long-term morphological evolution of coastal systems. Similar short-term exchange processes influencing the long-term morphologic evolution have been identified in other channel-shoal systems as well. For instance, the Dutch Ameland tidal inlet shows four phases of the cyclic evolution of channels and shoals with an alternation between one- and two-channel inlet configurations (Lenstra et al., 2019). In the Willapa Bay, Washington State, United States, a lateral circulation is observed to transport sediment from channel to the shoal which explains the turbid tidal edge (Mariotti and Fagherazzi, 2012). Moreover, such sediment exchanges not only transport nutrients and therefore influence aquatic habitats but also affect wetlands and mangroves by changing spatial dispersal of sediment supply and biogeomorphic feedbacks (McLachlan et al., 2020; Temmink et al., 2022; Temmerman et al., 2023). Therefore, our understandings of sediment exchange, coupled with long-term monitoring and interpretations, provide valuable insights for sediment management and ecological development.

5. Conclusions

Sediment exchanges play an important role in channel siltation and delta development but many human interventions have disturbed the exchange. In this study, we systematically evaluate the sediment exchanges in the modified distributary channels in the mouth zone of the Yangtze Estuary covering two tidal flats- Hengsha flat and Jiuduan shoal and a heavily modified channel-North Passage. We use in-situ data including samples measured at stations in channels, on tidal flats, and on structures, as well as in transects to give a full view of the sediment exchange pattern. A calibrated 3D numerical model is used to understand the large-scale hydrodynamics with different human interventions.

We found that the residual sediment transport on Jiuduan shoal is mainly landward with comparable lateral sediment exchanges particularly in tidal channels and near the South Passage. Sediment transport on the Hengsha flat indicates large sediment flux towards the channel and the landward and seaward residual transport is observed in the wet and dry season, respectively. Both flow and tidal asymmetry control the net landward sediment transport on tidal flats except for the dominant role of flow asymmetry in tidal channels in the wet season. On the other hand, the over-jetty flow induces residual sediment transport towards the channel from the Jiuduan shoal and off the channel to the Hengsha flat. The over-jetty sediment transport is mainly ascribed to water level gradients varying over tides in the channel-shoal system. In the channel, the residual sediment transport differs at tidal scale where the near-bed residual sediment transport is seaward at spring tide and landward at neap tide. Therefore, a residual circulation is identified between Jiuduan shoal and North Passage.

While the landward residual sediment transport in the channel is the strongest at neap tides in the wet season, this residual circulation is most pronounced at spring tides in the wet season contributing to the high siltation in the channel. This is one of the main reasons that high siltation maintains with reduced sediment supply and the combined role of

the weakened sediment exchange with insufficient sediment supply leads to the following decrease in siltation. More importantly, the construction of sediment barrier which blocks the sediment exchange between lower North Passage and Jiuduan shoal affect the large-scale delta evolution. We summarize three stages in which the 1st stage (2002–2010) promotes the growth of Hengsha flat and enhances the siltation in the channel; the 2nd stage (2010–2016) is the transition period with adjustment of tidal flats to insufficient sediment supply; the 3rd stage is accelerated by the blocking sediment barrier which promotes the growth of the Jiuduan shoal and therefore strengthens the southward growth of the delta.

In conclusion, the sediment exchange in the channel-shoal system of the Yangtze Estuary has been greatly altered to influence the shoal development and channel siltation, which is important for the future management of distributary delta systems with human interventions.

CRediT authorship contribution statement

Chunyan Zhu: Writing – original draft, Visualization, Validation, Investigation, Funding acquisition. **D.S. van Maren:** Writing – review & editing, Supervision, Methodology, Conceptualization. **Leicheng Guo:** Writing – review & editing, Methodology. **Weiming Xie:** Writing – review & editing, Investigation. **Chaofeng Xing:** Visualization, Investigation. **Zheng Bing Wang:** Writing – review & editing, Conceptualization. **Qing He:** Supervision, Resources, Project administration, Funding acquisition, Data curation, Conceptualization.

Declaration of competing interest

The authors declare that they have no known competing financial interests or personal relationships that could have appeared to influence the work reported in this paper.

Acknowledgements

This paper is financially supported by NSFC (Nos. U2040216, 42206169, 42106163), Shanghai Pujiang Program (22PJD020), China Postdoctoral Science Foundation (2022 M721165, 2023 T160219), and Shanghai Committee of Science and Technology (Nos. 20DZ1204700; 21230750600).

Open Research

Data are publicly available at https://figshare.com/s/7dd601b22e966ed922f7.

Appendix A. Supplementary data

Supplementary data to this article can be found online at https://doi.org/10.1016/j.catena.2025.108729.

Data availability

Data are publicly available at https://figshare.com/s/7dd601b22e966ed922f7.

References

Alebregtse, N.C., de Swart, H.E., 2016. Effect of river discharge and geometry on tides and net water transport in an estuarine network, an idealized model applied to the Yangtze Estuary. Cont. Shelf Res. 123, 29–49. https://doi.org/10.1016/j.csr.2016.03.028.

Burchard, H., Schuttelaars, H.M., Ralston, D.K., 2018. Sediment Trapping in Estuaries. Annu. Rev. Mar. Sci. 10, 371–395. https://doi.org/10.1146/annurev-marine-010816-060535.

Byun, D.-S., Hart, D.E., 2022. Tidal current classification insights for search, rescue and recovery operations in the Yellow and East China Seas and Korea Strait. Cont. Shelf Res. 232, 104632. https://doi.org/10.1016/j.csr.2021.104632.

Chen, L., Gong, W., Zhang, H., Zhu, L., Cheng, W., 2020a. Lateral Circulation and Associated Sediment Transport in a Convergent Estuary. JGR Oceans 125, e2019JC015926. https://doi.org/10.1029/2019JC015926.

Chen, Y., He, Q., Shen, J., Du, J., 2020b. The alteration of lateral circulation under the influence of human activities in a multiple channel system, Changjiang Estuary. Estuar. Coast. Shelf Sci. 242, 106823. https://doi.org/10.1016/j.ecss.2020.106823.

Chen, J., Zhu, H., Dong, Y., Sun, J., 1985. Development of the Changjiang estuary and its submerged delta. Continental Shelf Research, Sediment Dynamics of the Changjiang Estuary and the Adjacent East China Sea 4, 47–56. https://doi.org/10.1016/0278-4343(85)90021-4.

Edmonds, D.A., Slingerland, R.L., 2008. Stability of delta distributary networks and their bifurcations. Water Resour. Res. 44. https://doi.org/10.1029/2008WR006992.

Eidam, E.F., Sutherland, D.A., Ralston, D.K., Conroy, T., Dye, B., 2021. Shifting Sediment Dynamics in the Coos Bay Estuary in Response to 150 Years of Modification. JGR Oceans 126, e2020JC016771. https://doi.org/10.1029/2020JC016771.

Fu, G., 2013. Recent changes of tidal characteristics in the Yangtze Estuary, Port and Waterway Engineering, 11, 61-69 (Chinese with Abstract in English).

Geyer, W.R., MacCready, P., 2014. The Estuarine Circulation. Annu. Rev. Fluid Mech. 46, 175–197. https://doi.org/10.1146/annurev-fluid-010313-141302.

Gong, W., Zhang, G., Yuan, L., Zhang, H., Zhu, L., 2021. Effect of the Coriolis Force on Salt Dynamics in Convergent Partially Mixed Estuaries. JGR Oceans 126, e2021JC017391. https://doi.org/10.1029/2021JC017391.

Guo, X., Fan, D., Zheng, S., Wang, H., Zhao, B., Qin, C., 2021b. Revisited sediment budget with latest bathymetric data in the highly altered Yangtze (Changjiang) Estuary. Geomorphology 391, 107873. https://doi.org/10.1016/j.geomorph.2021.107873.

Guo, L., Zhu, C., Xie, W., Xu, F., Wu, H., Wan, Y., Wang, Z., Zhang, W., Shen, J., Wang, Z. B., He, Q., 2021a. Changjiang Delta in the Anthropocene: Multi-scale hydro-morphodynamics and management challenges. Earth Sci. Rev. 223, 103850. https://doi.org/10.1016/j.earscirev.2021.103850.

Guo, L., Xie, W., Xu, F., Wang, X., Zhu, C., Meng, Y., Zhang, W., He, Q., 2022. A historical review of sediment export–import shift in the North Branch of Changjiang Estuary. Earth Surf Processes Landf 47, 5–16. https://doi.org/10.1002/esp.5084.

Hiatt, M., Addink, E.A., Kleinhans, M.G., 2022. Connectivity and directionality in estuarine channel networks. Earth Surf Processes Landf 47, 807–824. https://doi.org/10.1002/esp.5286.

Hoitink, A.J.F., Nittrouer, J.A., Passalacqua, P., Shaw, J.B., Langendoen, E.J., Huismans, Y., van Maren, D.S., 2020. Resilience of River Deltas in the Anthropocene. JGR Earth Surface 125, e2019JF005201. https://doi.org/10.1029/2019JF005201.

Jeuken, M.C.J.L., Wang, Z.B., 2010. Impact of dredging and dumping on the stability of ebb–flood channel systems. Coast. Eng. 57, 553–566. https://doi.org/10.1016/j.coastaleng.2009.12.004.

Jiang, C., de Swart, H.E., Li, J., Liu, G., 2013. Mechanisms of along-channel sediment transport in the North Passage of the Yangtze Estuary and their response to large-scale interventions. Ocean Dyn. 63, 283–305. https://doi.org/10.1007/s10236-013-0594-4.

Juez, C., Garijo, N., Hassan, M.A., Nadal-Romero, E., 2021. Intraseasonal-to-Interannual analysis of discharge and suspended sediment concentration time-series of the upper changjiang (Yangtze river). Water Resour. Res. 57 (8) p. e2020WR029457.

Kakani, N.R., 2006. Coastal morphodynamics and asymmetric development of the Godavari delta: Implications to facies architecture and reservoir heterogeneity. J. Geol. Soc. India 67, 609–617.

Korus, J.T., Fielding, C.R., 2015. Asymmetry in Holocene river deltas: Patterns, controls, and stratigraphic effects. Earth Sci. Rev. 150, 219–242. https://doi.org/10.1016/j.earscirev.2015.07.013.

Lacy, J.R., Gladding, S., Brand, A., Collignon, A., Stacey, M., 2014. Lateral Baroclinic Forcing Enhances Sediment Transport from Shallows to Channel in an Estuary. Estuar. Coasts 37, 1058–1077. https://doi.org/10.1007/s12237-013-9748-3.

Larsen, L.H., Cannon, G.A., Choi, B.H., 1985. East China Sea tide currents. Continental Shelf Research, Sediment Dynamics of the Changjiang Estuary and the Adjacent East China Sea 4, 77–103. https://doi.org/10.1016/0278-4343(85)90023-8.

Lenstra, K.J.H., Pluis, S.R.P.M., Ridderinkhof, W., Ruessink, G., van der Vegt, M., 2019. Cyclic channel-shoal dynamics at the Ameland inlet: the impact on waves, tides, and sediment transport. Ocean Dyn. 69, 409–425. https://doi.org/10.1007/s10236-019-01249-3.

Li, M., Chen, Z., Yin, D., Chen, J., Wang, Z., Sun, Q., 2011. Morphodynamic characteristics of the dextral diversion of the Yangtze River mouth, China: tidal and the Coriolis Force controls. Earth Surf Processes Landf 36, 641–650. https://doi.org/10.1002/esp.2082.

Li, Y., Jia, J., Zhu, Q., Cheng, P., Gao, S., Wang, Y.P., 2018. Differentiating the effects of advection and resuspension on suspended sediment concentrations in a turbid estuary. Marine Geology 403, 179–190. https://doi.org/10.1016/j.margeo.2018.06.001.

Li, J., Zhang, C., 1998. Sediment resuspension and implications for turbidity maximum in the Changjiang Estuary. Mar. Geol. 148, 117–124. https://doi.org/10.1016/S0025-3227(98)00003-6.

Li, X., Zhu, J., Yuan, R., Qiu, C., Wu, H., 2016. Sediment trapping in the Changjiang Estuary: Observations in the North Passage over a spring-neap tidal cycle. Estuar. Coast. Shelf Sci. 177, 8–19. https://doi.org/10.1016/j.ecss.2016.05.004.

Lin, J., van Prooijen, B.C., Guo, L., Zhu, C., He, Q., Wang, Z.B., 2021. Regime shifts in the Changjiang (Yangtze River) Estuary: The role of concentrated benthic suspensions. Mar. Geol. 433, 106403. https://doi.org/10.1016/j.margeo.2020.106403.

Liu, Y., Reible, D., Hussain, F., 2022. Roles of Tidal Cycling, Hyporheic Exchange and Bioirrigation on Metal Release From Estuary Sediments. Water Resour. Res. 58, e2021WR030790. https://doi.org/10.1029/2021WR030790.

Liu, G., Zhu, J., Wang, Y., Wu, H., Wu, J., 2011. Tripod measured residual currents and sediment flux: Impacts on the silting of the Deepwater Navigation Channel in the

Changjiang Estuary. Estuar. Coast. Shelf Sci. 93, 192–201. https://doi.org/10.1016/j.ecss.2010.08.008.
Lu, S., Tong, C., Lee, D., Zheng, J., Shen, J., Zhang, W., Yan, Y., 2015. Propagation of tidal waves up in Yangtze Estuary during the dry season. J. Geophys. Res. Oceans 120, 6445–6473. https://doi.org/10.1002/2014JC010414.
Luo, W., Shen, F., He, Q., Cao, F., Zhao, H., Li, M., 2022. Changes in suspended sediments in the Yangtze River Estuary from 1984 to 2020: Responses to basin and estuarine engineering constructions. Sci. Total Environ. 805, 150381. https://doi.org/10.1016/j.scitotenv.2021.150381.
Mariotti, G., Fagherazzi, S., 2012. Channels-tidal flat sediment exchange: The channel spillover mechanism. Journal of Geophysical Research: Oceans 117 (C3).
McLachlan, R.L., Ogston, A.S., Asp, N.E., Fricke, A.T., Nittrouer, C.A., Gomes, V.J.C., 2020. Impacts of tidal-channel connectivity on transport asymmetry and sediment exchange with mangrove forests. Estuar. Coast. Shelf Sci. 233, 106524.
Nidzieko, N.J., Ralston, D.K., 2012. Tidal asymmetry and velocity skew over tidal flats and shallow channels within a macrotidal river delta. J. Geophys. Res. 117. https://doi.org/10.1029/2011JC007384.
Nienhuis, J.H., Ashton, A.D., Edmonds, D.A., Hoitink, A.J.F., Kettner, A.J., Rowland, J. C., Törnqvist, T.E., 2020. Global-scale human impact on delta morphology has led to net land area gain. Nature 577, 514–518. https://doi.org/10.1038/s41586-019-1905-9.
Pearson, S.G., van Prooijen, B.C., Elias, E.P.L., Vitousek, S., Wang, Z.B., 2020. Sediment Connectivity: A Framework for Analyzing Coastal Sediment Transport Pathways. JGR Earth Surface 125, e2020JF005595. https://doi.org/10.1029/2020JF005595.
Ralston, D.K., Geyer, W.R., Warner, J.C., 2012. Bathymetric controls on sediment transport in the Hudson River estuary: Lateral asymmetry and frontal trapping. J. Geophys. Res. 117, n/a-n/a. https://doi.org/10.1029/2012JC008124.
Seo, J.Y., Kim, Y.H., Ryu, J., Ha, H.K., 2023. Wind-induced switch of estuarine residual circulations and sediment transport in microtidal bay. Estuar. Coast. Shelf Sci. 288, 108371. https://doi.org/10.1016/j.ecss.2023.108371.
Song, D., Wang, X.H., Liang, H., Kuang, C., Olabarrieta, M., Gu, J., Song, H., Dong, Z., Huijts, K.M.H., Schuttelaars, H.M., de Swart, H.E., Valle-Levinson, A., 2013. Suspended sediment transport in the Deepwater Navigation Channel, Yangtze River Estuary, China, in the dry season 2009: 2. Numerical simulations. J. Geophys. Res. Oceans 118, 5568–5590. https://doi.org/10.1002/jgrc.20411.
Speer, P.E., Aubrey, D.G., 1985. A study of non-linear tidal propagation in shallow inlet/estuarine systems Part II: Theory. Estuar. Coast. Shelf Sci. 21, 207–224. https://doi.org/10.1016/0272-7714(85)90097-6.
Temmerman, S., Horstman, E.M., Krauss, K.W., Mullarney, J.C., Pelckmans, I., Schoutens, K., 2023. Marshes and mangroves as nature-based coastal storm buffers. Ann. Rev. Mar. Sci. 15 (1), 95–118.
Temmink, R.J., Lamers, L.P., Angelini, C., Bouma, T.J., Fritz, C., van de Koppel, J., Lexmond, R., Rietkerk, M., Silliman, B.R., Joosten, H., van der Heide, T., 2022. Recovering wetland biogeomorphic feedbacks to restore the world's biotic carbon hotspots. Science 376 (6593), p.eabn1479.
van Maren, D.S., Winterwerp, J.C., Vroom, J., 2015. Fine sediment transport into the hyper-turbid lower Ems River: the role of channel deepening and sediment-induced drag reduction. Ocean Dyn. 65, 589–605. https://doi.org/10.1007/s10236-015-0821-2.
van Maren, D.S., Beemster, J.G.W., Wang, Z.B., Khan, Z.H., Schrijvershof, R.A., Hoitink, A.J.F., 2023a. Tidal amplification and river capture in response to land reclamation in the Ganges-Brahmaputra delta. Catena 220, 106651. https://doi.org/10.1016/j.catena.2022.106651.
van Maren, D.S., Maushake, C., Mol, J.-W., van Keulen, D., Jürges, J., Vroom, J., Schuttelaars, H., Gerkema, T., Schulz, K., Badewien, T.H., Gerriets, M., Engels, A., Wurpts, A., Oberrecht, D., Manning, A.J., Bailey, T., Ross, L., Mohrholz, V., Horemans, D.M.L., Becker, M., Post, D., Schmidt, C., Dankers, P.J.T., 2023b. Synoptic observations of sediment transport and exchange mechanisms in the turbid Ems Estuary: the EDoM campaign. Earth Syst. Sci. Data 15, 53–73. https://doi.org/10.5194/essd-15-53-2023.
Walters, R.A., Heston, C., 1982. Removing Tidal-Period Variations from Time-Series Data Using Low-Pass Digital Filters. J. Phys. Oceanogr. 12, 112–115.
Wan, Y., Roelvink, D., Li, W., Qi, D., Gu, F., 2014. Observation and modeling of the storm-induced fluid mud dynamics in a muddy-estuarine navigational channel. Geomorphology 217, 23–36. https://doi.org/10.1016/j.geomorph.2014.03.050.
Wang, J., Chu, A., Dai, Z., Nienhuis, J., 2024. Delft3D model-based estuarine suspended sediment budget with morphodynamic changes of the channel-shoal complex in a mega fluvial-tidal delta. Eng. Appl. Comput. Fluid Mech. 18, 2300763. https://doi.org/10.1080/19942060.2023.2300763.
Wang, Z.B., Jeuken, M.C.J.L., Gerritsen, H., de Vriend, H.J., Kornman, B.A., 2002. Morphology and asymmetry of the vertical tide in the Westerschelde estuary. Cont. Shelf Res. 22, 2599–2609. https://doi.org/10.1016/S0278-4343(02)00134-6.
Winterwerp, J.C., Wang, Z.B., 2013. Man-induced regime shifts in small estuaries—I: theory. Ocean Dyn. 63, 1279–1292. https://doi.org/10.1007/s10236-013-0662-9.
Wu, H., Zhu, J., Choi, B.H., 2010. Links between saltwater intrusion and subtidal circulation in the Changjiang Estuary: A model-guided study. Cont. Shelf Res. 30, 1891–1905. https://doi.org/10.1016/j.csr.2010.09.001.
Xie, D., Pan, C., Wu, X., Gao, S., Wang, Z.B., 2017a. Local human activities overwhelm decreased sediment supply from the Changjiang River: Continued rapid accumulation in the Hangzhou Bay-Qiantang Estuary system. Mar. Geol. 392, 66–77. https://doi.org/10.1016/j.margeo.2017.08.013.
Xie, D., Pan, C., Wu, X., Gao, S., Wang, Z., 2017b. The variations of sediment transport patterns in the outer Changjiang Estuary and Hangzhou B ay over the last 30 years. J. Geophys. Res. Oceans 122 (4), 2999–3020.
Zhang, W., Cao, Y., Zhu, Y., Zheng, J., Ji, X., Xu, Y., Wu, Y., Hoitink, A.J.F., 2018. Unravelling the causes of tidal asymmetry in deltas. J. Hydrol. 564, 588–604. https://doi.org/10.1016/j.jhydrol.2018.07.023.
Zhang, D., Xie, W., Shen, J., Guo, L., Chen, Y., He, Q., 2022. Sediment dynamics in the mudbank of the Yangtze River Estuary under regime shift of source and sink. Int. J. Sedim. Res. 37, 97–109. https://doi.org/10.1016/j.ijsrc.2021.07.005.
Zhou, Z., Coco, G., Townend, I., Olabarrieta, M., van der Wegen, M., Gong, Z., D'Alpaos, A., Gao, S., Jaffe, B.E., Gelfenbaum, G., He, Q., Wang, Y., Lanzoni, S., Wang, Z., Winterwerp, H., Zhang, C., 2017. Is "Morphodynamic Equilibrium" an oxymoron? Earth-Science Reviews 165, 257–267. https://doi.org/10.1016/j.earscirev.2016.12.002.
Zhou, Z., Ge, J., van Maren, D.S., Wang, Z.B., Kuai, Y., Ding, P., 2021. Study of Sediment Transport in a Tidal Channel-Shoal System: Lateral Effects and Slack-Water Dynamics. Journal of Geophysical Research: Oceans 126, e2020JC016334. https://doi.org/10.1029/2020JC016334.
Zhu, C., Guo, L., van Maren, D.S., Tian, B., Wang, X., He, Q., Wang, Z.B., 2019. Decadal morphological evolution of the mouth zone of the Yangtze Estuary in response to human interventions. Earth Surf Processes Landf 44, 2319–2332. https://doi.org/10.1002/esp.4647.
Zhu, C., Guo, L., van Maren, D.S., Wang, Z.B., He, Q., 2021a. Exploration of Decadal Tidal Evolution in Response to Morphological and Sedimentary Changes in the Yangtze Estuary. JGR. Oceans 126, e2020JC017019. https://doi.org/10.1029/2020JC017019.
Zhu, C., van Maren, D.S., Guo, L., Lin, J., He, Q., Wang, Z.B., 2021b. Effects of Sediment-Induced Density Gradients on the Estuarine Turbidity Maximum in the Yangtze Estuary. JGR. Oceans 126, e2020JC016927. https://doi.org/10.1029/2020JC016927.
Zhu, C., van Maren, D.S., Guo, L., Lin, J., He, Q., Wang, Z.B., 2022. Feedback Effects of Sediment Suspensions on Transport Mechanisms in an Estuarine Turbidity Maximum. JGR. Oceans 127, e2021JC018029. https://doi.org/10.1029/2021JC018029.
Zhu, C., Dong, J., Xie, W., Guo, L., He, Q., 2024. Multi-fraction sediment transport in the turbidity maximum of the Yangtze Estuary during the extreme flood. Mar. Sci. Bull. 43 (03), 335–345 in Chinese with Abstract in English.
Zhu, L., He, Q., Shen, J., Wang, Y., 2016. The influence of human activities on morphodynamics and alteration of sediment source and sink in the Changjiang Estuary. Geomorphology 273, 52–62. https://doi.org/10.1016/j.geomorph.2016.07.025.